

## ORIGINAL RESEARCH

# Theoretical equilibrium lead(II) solubility revisited: Open source code and practical relationships

David G. Wahman<sup>1</sup>  | Matthew D. Pinelli<sup>2</sup>  | Michael R. Schock<sup>1</sup>  |  
Darren A. Lytle<sup>1</sup> 

<sup>1</sup>United States Environmental Protection Agency, Office of Research & Development, Cincinnati, Ohio, USA

<sup>2</sup>Oak Ridge Associated Universities (ORAU) Contractor to USEPA, Cincinnati, Ohio, USA

## Correspondence

Darren A. Lytle, USEPA, 26 W. Martin Luther King Dr., Cincinnati, OH 45268, USA.

Email: lytle.darren@epa.gov

**Associate Editor:** Kimberly L. Jones

## Abstract

A theoretical equilibrium lead(II) (Pb(II)) solubility model coded in Fortran (LEADSOL) was updated and implemented in open source R code, verified against LEADSOL output, and used to simulate theoretical equilibrium total soluble Pb(II) (TOTSOLPb) concentrations under a variety of practical scenarios. The developed R code file (app.R) is publicly available for download at GitHub (<https://github.com/USEPA/TELSS>) along with instructions to run the R code locally, allowing the user to explore Pb(II) solubility by selecting desired simulation conditions (e.g., water quality, equilibrium constants, and Pb(II) solids to consider). In addition, the R code serves as a reproducible baseline for alternative model development and future model improvements, allowing users to update, modify, and share the R code to meet their needs. Using the R code, several solubility diagrams were generated to highlight practical relationships related to TOTSOLPb concentrations, including the impact of pH and dissolved inorganic carbon, orthophosphate, sulfate, and chloride concentrations.

## KEYWORDS

chloride, DIC, lead, LEADSOL, phosphate, solubility model, sulfate, TELSS

## 1 | INTRODUCTION

Minimizing lead (Pb) release in drinking water distribution systems (DWDSs) from Pb pipes, brass fixtures, Pb-based solders, and galvanic connections is a public health goal of all water utilities as there is no safe Pb level, indicated by the US Environmental Protection Agency's (EPA) maximum contaminant level goal (MCLG) of 0 mg/L for Pb (Federal Register, 1991b). The EPA's Lead and Copper Rule (LCR), which is currently under review (<https://www.epa.gov/sdwa/lead-and-copper-rule-long-term-revisions>), established an action level for Pb at the consumer's tap of 0.015 mg/L in a one-liter first draw sample (Federal Register, 1992, 1991a, 1991b). Since the LCR's promulgation, the understanding of relationships between water quality and the solubility of

Pb-containing minerals found in DWDSs has grown extensively. The impacts of factors such as pH, dissolved inorganic carbon (DIC), and orthophosphate on the solubility of Pb solids are relatively well known (Hunt & Creasey, 1980; Schock et al., 1996; Schock & Clement, 1998; Schock & Gardels, 1983; Schock & Lytle, 2011; Schock & Wagner, 1985; Sheiham & Jackson, 1981). These relationships have been described theoretically according to fundamental solubility models (e.g., Schock, 1980, 1981, 1989; Schock et al., 1996) and served as the primary historical basis for Pb reduction strategies in drinking water and, therefore, risk reduction from exposure to Pb (United States Environmental Protection Agency, 2019).

The existing conventional wisdom governing Pb solubility and the formation of Pb passivation scales is largely

based on a combination of equilibrium solubility modeling computations, laboratory/pilot-scale experimental studies, and field sampling (Dodrill & Edwards, 1995; Edwards et al., 1999; Jackson & Sheiham, 1980; Schock, 1980, 1981, 1989; Schock et al., 1996; Tully et al., 2019). Solubility models simulate dissolved Pb (and other chemical) concentrations, assuming thermodynamic equilibrium or prolonged metastability with various Pb solid phases and have provided guidance regarding which mineral phases are simulated to control Pb release through the formation of passivating films in a given aqueous environment (Hunt & Creasey, 1980; Jackson & Sheiham, 1980; Schock, 1980, 1989; Schock et al., 1996; Schock & Clement, 1998; Schock & Gardels, 1983; Schock & Lytle, 2011; Schock & Sandvig, 2004; Sheiham & Jackson, 1981).

Over the past several decades, however, research and field observations have revealed the complexity of mechanisms associated with Pb release and corrosion control where factors beyond theoretical solubility considerations also play important roles in determining Pb concentrations in drinking water, including pipe scale age, structure, and composition (e.g., Tully et al., 2019), hydraulic and mass transfer considerations (e.g., Ma et al., 2019), biological activity/biofilm (e.g., Zhang et al., 2009), and particulate Pb (e.g., Del Toral et al., 2013). Because of this inherent complexity, there are many tools available to water utilities for assessing and improving Pb corrosion control to minimize Pb concentrations in drinking water from leaded sources (e.g., Pb service lines, Pb-based solders, and brasses), and no single approach can be relied upon in isolation. These tools include pipe rigs (Economic and Engineering Services, 1990; Kirmeyer et al., 1994; Williams et al., 2018), coupon studies (Schneider et al., 2007), pipe scale analyses (Tully et al., 2019), and theoretical Pb solubility modeling (Schock et al., 1996). The focus herein is on theoretical Pb(II) solubility modeling.

Although Pb solubility modeling is based on a fundamental approach to simulate the total soluble Pb concentration in drinking water for a given water quality, very little advancement has been made in the drinking water field to make such models widely accessible to allow continued development, ease of evaluation, and a reproducible framework. Drinking water Pb solubility models are available pre-programmed in commercial software (e.g., Water!Pro, Schott, 1998), have been developed in computer codes such as Fortran (e.g., Schock, 1980, 1981, 1989; Schock et al., 1996), or implemented using various software, including MINEQL+ (e.g., Dodrill & Edwards, 1995; Edwards et al., 1999) or PHREEQC (e.g., Jurgens et al., 2019). In addition, other platforms are readily available where Pb solubility models could be implemented, including MINTEQA2 and Visual MINTEQA2 (Gustafsson, 2015), the Geochemist's Workbench (Bethke, 2010), and Microsoft Excel (Crouch & Holler, 2014). Even with these current options, there is no current Pb(II) solubility model widely

### Article Impact Statement

Based on LEADSOL, an open source lead(II) solubility model was developed and used to highlight practical lead(II) solubility relationships.

available in an open source format that can be acquired at no cost and does not require expertise in implementing the model or conducting simulations. As a result, the original published simulations generated with the LEADSOL model are commonly reproduced and used in presentations (e.g., Brandhuber, 2020), manuscripts (e.g., Brown et al., 2013), and industry manuals of practice (e.g., American Water Works Association, 2017) related to drinking water Pb solubility.

To address the need for an accessible Pb(II) solubility model and provide a tool to the drinking water industry, the current work created a theoretical Pb(II) solubility model using R code based on the previously verified and validated LEADSOL Fortran code originally developed in 1978 (Schock, 1980, 1981; Schock et al., 1996; Schock & Gardels, 1983). The current R implementation creates a free, open source Pb(II) solubility model for current use and continued development. A detailed description of the underlying Pb(II) solubility model and updates made from LEADSOL, verification against LEADSOL output, and discussion of several practical relationships from solubility diagrams generated using the R code are presented herein. In addition, the developed R code serves as an example for making additional solubility model code widely available in an open source format (e.g., copper(II) solubility model) and provides code segments that can be used in analyzing experimental data for future model expansion, refinement, and sharing. Furthermore, this work presents fresh perspectives on theoretical Pb(II) solubility by presenting new graphical presentations of relationships with pH, DIC, and orthophosphate. Finally, this work expanded previous modeling efforts to consider the impact of sulfate and chloride on Pb(II) solubility under acidic conditions, an environment relevant to galvanic corrosion (i.e., Pb-based solders). The theoretical Pb(II) solubility model code and new presentation and discussion of model output provides the drinking water industry with a practical research tool and reference materials.

## 2 | PB(II) SOLUBILITY MODEL DEVELOPMENT

### 2.1 | Pb(II) solubility equilibria and equilibrium constants

An existing theoretical equilibrium Pb(II) solubility model (Schock et al., 1996) was implemented in R (R Core

**TABLE 1** Baseline theoretical lead(II) solubility model equilibria and constants (log K) at 25°C and 0 M ionic strength

Name	Equilibrium	Log K	Reference
<b>Solids to consider</b>			
$K_{\text{solid}}$ (Lead Hydroxide)	$\text{Pb}(\text{OH})_2 (\text{s}) + 2\text{H}^+ \rightleftharpoons \text{Pb}^{2+} + 2\text{H}_2\text{O}$	13.06	Schock et al. (1996)
$K_{\text{solid}}$ (Cerussite)	$\text{PbCO}_3 (\text{s}) \rightleftharpoons \text{Pb}^{2+} + \text{CO}_3^{2-}$	-13.11	Schock et al. (1996)
$K_{\text{solid}}$ (Hydrocerussite)	$\text{Pb}_3(\text{CO}_3)_2(\text{OH})_2 (\text{s}) + 2\text{H}^+ \rightleftharpoons 3\text{Pb}^{2+} + 2\text{CO}_3^{2-} + 2\text{H}_2\text{O}$	-18.00	Schock et al. (1996)
$K_{\text{solid}}$ (Hydroxypyromorphite)	$\text{Pb}_5(\text{PO}_4)_3\text{OH} (\text{s}) + \text{H}^+ \rightleftharpoons 5\text{Pb}^{2+} + 3\text{PO}_4^{3-} + \text{H}_2\text{O}$	-62.83	Schock et al. (1996)
$K_{\text{solid}}$ (Pyromorphite)	$\text{Pb}_5(\text{PO}_4)_3\text{Cl} (\text{s}) \rightleftharpoons 5\text{Pb}^{2+} + 3\text{PO}_4^{3-} + \text{Cl}^-$	-79.6	Topolska et al. (2016)
$K_{\text{solid}}$ (primary lead orthophosphate)	$\text{Pb}(\text{H}_2\text{PO}_4)_2 (\text{s}) \rightleftharpoons \text{Pb}^{2+} + 2\text{PO}_4^{3-} + 4\text{H}^+$	-48.916	Powell et al. (2009)
$K_{\text{solid}}$ (secondary lead orthophosphate)	$\text{PbHPO}_4 (\text{s}) \rightleftharpoons \text{Pb}^{2+} + \text{PO}_4^{3-} + \text{H}^+$	-23.81	Schock et al. (1996)
$K_{\text{solid}}$ (tertiary lead orthophosphate)	$\text{Pb}_3(\text{PO}_4)_2 (\text{s}) \rightleftharpoons 3\text{Pb}^{2+} + 2\text{PO}_4^{3-}$	-44.4	Powell et al. (2009)
$K_{\text{solid}}$ (anglesite)	$\text{PbSO}_4 (\text{s}) \rightleftharpoons \text{Pb}^{2+} + \text{SO}_4^{2-}$	-7.79	Schock et al. (1996)
$K_{\text{solid}}$ (laurionite)	$\text{PbClOH} (\text{s}) + \text{H}^+ \rightleftharpoons \text{Pb}^{2+} + \text{Cl}^- + \text{H}_2\text{O}$	0.619	Nasanen and Lindell (1976)
<b>Hydroxide complexes</b>			
$\beta_{1,\text{OH}}$	$\text{Pb}^{2+} + \text{H}_2\text{O} \rightleftharpoons \text{PbOH}^+ + \text{H}^+$	-7.22	Schock et al. (1996)
$\beta_{2,\text{OH}}$	$\text{Pb}^{2+} + 2\text{H}_2\text{O} \rightleftharpoons \text{Pb}(\text{OH})_2 (\text{aq}) + 2\text{H}^+$	-16.91	Schock et al. (1996)
$\beta_{3,\text{OH}}$	$\text{Pb}^{2+} + 3\text{H}_2\text{O} \rightleftharpoons \text{Pb}(\text{OH})_3^- + 3\text{H}^+$	-28.08	Schock et al. (1996)
$\beta_{4,\text{OH}}$	$\text{Pb}^{2+} + 4\text{H}_2\text{O} \rightleftharpoons \text{Pb}(\text{OH})_4^{2-} + 4\text{H}^+$	-39.72	Schock et al. (1996)
$\beta_{2,1,\text{OH}}$	$2\text{Pb}^{2+} + \text{H}_2\text{O} \rightleftharpoons \text{Pb}_2\text{OH}^{3+} + \text{H}^+$	-6.36	Schock et al. (1996)
$\beta_{3,4,\text{OH}}$	$3\text{Pb}^{2+} + 4\text{H}_2\text{O} \rightleftharpoons \text{Pb}_3(\text{OH})_4^{2+} + 4\text{H}^+$	-23.86	Schock et al. (1996)
$\beta_{4,4,\text{OH}}$	$4\text{Pb}^{2+} + 4\text{H}_2\text{O} \rightleftharpoons \text{Pb}_4(\text{OH})_4^{4+} + 4\text{H}^+$	-20.88	Schock et al. (1996)
$\beta_{6,8,\text{OH}}$	$6\text{Pb}^{2+} + 8\text{H}_2\text{O} \rightleftharpoons \text{Pb}_6(\text{OH})_8^{4+} + 8\text{H}^+$	-43.62	Schock et al. (1996)
<b>Chloride complexes</b>			
$K_{1,\text{Cl}}$	$\text{Pb}^{2+} + \text{Cl}^- \rightleftharpoons \text{PbCl}^+$	1.59	Schock et al. (1996)
$\beta_{2,\text{Cl}}$	$\text{Pb}^{2+} + 2\text{Cl}^- \rightleftharpoons \text{PbCl}_2 (\text{aq})$	1.80	Schock et al. (1996)
$\beta_{3,\text{Cl}}$	$\text{Pb}^{2+} + 3\text{Cl}^- \rightleftharpoons \text{PbCl}_3^-$	1.71	Schock et al. (1996)
$\beta_{4,\text{Cl}}$	$\text{Pb}^{2+} + 4\text{Cl}^- \rightleftharpoons \text{PbCl}_4^{2-}$	1.43	Schock et al. (1996)
<b>Sulfate complexes and acid-base</b>			
$K_{\text{S}}$	$\text{HSO}_4^- \rightleftharpoons \text{SO}_4^{2-} + \text{H}^+$	-1.99	Benjamin (2002)
$K_{1,\text{SO}_4}$	$\text{Pb}^{2+} + \text{SO}_4^{2-} \rightleftharpoons \text{PbSO}_4 (\text{aq})$	2.73	Schock et al. (1996)
$\beta_{2,\text{SO}_4}$	$\text{Pb}^{2+} + 2\text{SO}_4^{2-} \rightleftharpoons \text{Pb}(\text{SO}_4)_2^{2-}$	3.50	Schock et al. (1996)
<b>Carbonate complexes and acid-base</b>			
$K_{\text{c1}}$	$\text{H}_2\text{CO}_3^* \rightleftharpoons \text{HCO}_3^- + \text{H}^+$	-6.355	Powell et al. (2005)
$K_{\text{c2}}$	$\text{HCO}_3^- \rightleftharpoons \text{H}^+ + \text{CO}_3^{2-}$	-10.336	Powell et al. (2005)
$K_{1,\text{CO}_3}$	$\text{Pb}^{2+} + \text{H}^+ + \text{CO}_3^{2-} \rightleftharpoons \text{PbHCO}_3^+$	12.59	Schock et al. (1996)
$K_{2,\text{CO}_3}$	$\text{Pb}^{2+} + \text{CO}_3^{2-} \rightleftharpoons \text{PbCO}_3 (\text{aq})$	7.10	Schock et al. (1996)
$K_{3,\text{CO}_3}$	$\text{Pb}^{2+} + 2\text{CO}_3^{2-} \rightleftharpoons \text{Pb}(\text{CO}_3)_2^{2-}$	10.33	Schock et al. (1996)
<b>Phosphate complexes and acid-base</b>			
$K_{\text{p1}}$	$\text{H}_3\text{PO}_4 \rightleftharpoons \text{H}^+ + \text{H}_2\text{PO}_4^-$	-2.141	Powell et al. (2005)
$K_{\text{p2}}$	$\text{H}_2\text{PO}_4^- \rightleftharpoons \text{H}^+ + \text{HPO}_4^{2-}$	-7.200	Powell et al. (2005)
$K_{\text{p3}}$	$\text{HPO}_4^{2-} \rightleftharpoons \text{H}^+ + \text{PO}_4^{3-}$	-12.338	Powell et al. (2005)
$K_{1,\text{PO}_4}$	$\text{Pb}^{2+} + \text{H}^+ + \text{PO}_4^{3-} \rightleftharpoons \text{PbHPO}_4 (\text{aq})$	15.41	Schock et al. (1996)
$K_{2,\text{PO}_4}$	$\text{Pb}^{2+} + 2\text{H}^+ + \text{PO}_4^{3-} \rightleftharpoons \text{PbH}_2\text{PO}_4^+$	21.05	Schock et al. (1996)

Team, 2020) to create code that is freely available for download at GitHub (<https://github.com/USEPA/TELSS>) and can be run on a local computer or if the user desires shared online (e.g., <https://www.shinyapps.io/>). The R code is referred to as the Theoretical Equilibrium Lead Solubility Simulator (TELSS) and allows simulation of theoretical equilibrium total soluble Pb(II) (TOTSOLPb) concentrations under a variety of user-defined conditions (e.g., DIC, phosphate, sulfate, and chloride concentrations; pH; ionic strength; and various combinations of Pb(II) containing solids controlling solubility). The implemented baseline equilibria and associated equilibrium constants are summarized in Table 1.

In addition to maintaining the original functionality of LEADSOL (Schock et al., 1996), TELSS includes the following updates: (i) addition of laurionite,  $\text{PbClOH}$  (s), (Nasanen & Lindell, 1976) as additional Pb(II) solid (Table 1), (ii) implementation of (chloro)pyromorphite,  $\text{Pb}_5(\text{PO}_4)_3\text{Cl}$  (s), using a recent equilibrium constant estimate (Topolska et al., 2016), and (iii) inclusion of alternative equilibrium constants (Table 2) that have been published since Schock et al. (1996) for hydroxypyromorphite,  $\text{Pb}_5(\text{PO}_4)_3\text{OH}$  (s), (Zhu et al., 2015) and pyromorphite (Xie & Giammar, 2007) or are available in the literature for laurionite (Lothenbach et al., 1999). In addition, the TELSS code is setup in a flexible manner such that additional possible selections for equilibria and/or equilibrium constants can be implemented with minor modifications to the TELSS code if the user desires (see Supplementary Information (SI) *Relevant Code Chunks for a Solid (Anglesite Example)* and *Relevant Code Chunks for an Aqueous Complex ( $\text{PbSO}_4[\text{aq}]$  Example)*).

## 2.2 | Activity corrections

To determine the concentration-based equilibrium constants, the user-selected ionic strength ( $\mu$ ) is used to calculate required activity coefficients ( $\gamma_z$ ) from the Davies equation using Equation (1) (Benjamin, 2002) where  $z$  is the ion charge. In Equation (1), the Debye-Hückel constant ( $A_{\text{DH}}$ ) is determined from Equation (2) at the specified temperature in Kelvin ( $T_K$ ) (Benjamin, 2002), and in Equation (3), the dielectric constant for water ( $\epsilon_{\text{water}}$ ) is determined at the specified temperature in  $^{\circ}\text{C}$  ( $T_c$ ) from Equation (3) (Malmberg & Maryott, 1956). Currently, the TELSS code fixes the temperature at  $25^{\circ}\text{C}$  (298.15 K), but this could become another user-selected variable when temperature dependence of all the equilibria is determined.

$$\log \gamma_z = -A_{\text{DH}} z^2 \left( \frac{\sqrt{\mu}}{1 + \sqrt{\mu}} - 0.3\mu \right) = -0.51 z^2 \left( \frac{\sqrt{\mu}}{1 + \sqrt{\mu}} - 0.3\mu \right) @ 25^{\circ}\text{C} \quad (1)$$

$$A_{\text{DH}} = 1.82 \times 10^6 (\epsilon_{\text{water}} T_K)^{-3/2} = 0.51 @ 25^{\circ}\text{C} \quad (2)$$

TABLE 2 Alternative lead(II) solubility model equilibrium constants (log K) available for selection

Name	Log K	Reference
$K_{\text{solid}}$ (hydroxypyromorphite)	−66.77	Zhu et al. (2015)
$K_{\text{solid}}$ (pyromorphite)	−80.4	Xie and Giammar (2007)
$K_{\text{solid}}$ (laurionite)	0.29	Lothenbach et al. (1999)

$$\begin{aligned} \epsilon_{\text{water}} &= 87.740 - 0.40008T_c + 9.398 \times 10^{-4}T_c^2 - 1.410 \times 10^{-6}T_c^3 \\ &= 78.3 @ 25^{\circ}\text{C}. \end{aligned} \quad (3)$$

## 2.3 | General solution methodology

All simulations are only valid for  $25^{\circ}\text{C}$  and only for Pb(II). To solve the equilibria presented in Table 1 and estimate dissolved chemical concentrations, several user-selected initial conditions are required: (i) pH; (ii) ionic strength; (iii) dissolved (a) inorganic carbon (DIC), (b) total inorganic phosphate ( $\text{TOTPO}_4$ ), (c) chloride, and (d) total inorganic sulfate ( $\text{TOTSO}_4$ ) concentrations; (iv) solids to include in the multiple solids analysis; and (v) equilibrium constant values, if multiple choices exist.

Using the user-selected conditions, a solution of the model progresses through the following general steps that are further detailed in the SI *Derivation of Solubility Model Solution* for each possible solid:

1. Inorganic carbon acid–base species concentrations are calculated.
2. Inorganic phosphate acid–base species concentrations are calculated.
3. Inorganic sulfate acid–base species concentrations are calculated.
4. Pb(II) ion ( $\text{Pb}^{2+}$ ) concentration is calculated.
5. Various aqueous Pb(II) complex concentrations (hydroxide, chloride, sulfate, carbonate, and phosphate) are calculated.

Once all the soluble chemical species concentrations are determined, various solubility diagrams are created, including an overall solubility diagram that considers all the user-selected Pb(II) solids to consider.

## 2.4 | TELSS code and graphical user interface

Instructions for acquiring and running the TELSS code are provided in the SI *Instructions for Acquiring and Running TELSS R Code*. Running the TELSS code provides a locally

running interactive application for the user to simulate TOTSOLPb concentrations, containing a graphical user interface (GUI) developed using the R Shiny package (Chang et al., 2020). In an improvement from LEADSOL, the GUI allows interactive selection of simulation conditions and generation of desired outputs of TOTSOLPb concentrations versus selected parameters (e.g., pH, phosphate, and DIC). Furthermore, the simulation results are exportable as a comma separated variable file (.csv). A detailed description of the GUI is provided in the SI *Graphical User Interface Description*.

## 2.5 | Model verification

In addition to making every effort to consistently convert the original Fortran code into R, it was important in this work to verify the TELSS code implementation by comparing conditions and associated outputs to LEADSOL simulations (Schock, 1980, 1981; Schock et al., 1996) given the widespread acceptance and use of the related relationships by the drinking water industry. To verify the implementation of the TELSS code, TELSS simulations were verified against identical simulations (i.e., initial conditions, equilibria, and equilibrium constants) generated using the Schock et al. (1996) LEADSOL code. In addition, a Microsoft Excel-based implementation of the solubility model was used to further verify numerical implementation. Two general scenarios were simulated to compare LEADSOL and TELSS: conditions (i) without and (ii) with phosphate (Figures S9–S11). The TELSS simulations agreed with the LEADSOL simulations. In addition, comparisons of TELSS output with a Microsoft Excel-based model implementation output were numerically identical for each simulated chemical species for various simulations (22 total): 100 mg Cl/L chloride, 100 mg SO<sub>4</sub>/L sulfate, 2 mg PO<sub>4</sub>/L orthophosphate, 10 mg C/L DIC, 5 mM ionic strength, pHs 6 and 11, and 11 different solid conditions (each of the 10 possible solids included individually and an additional simulation where all 10 possible solids were considered). Therefore, the TELSS code implementation was verified.

## 2.6 | Model limitations

In general, Pb(II) solubility models are useful tools to simulate the theoretical equilibrium TOTSOLPb concentrations in drinking water, but they should be used in combination with other tools for estimating potential TOTSOLPb concentrations in real systems due to the complexity of factors that impact actual Pb concentrations in DWDSs. Acknowledging the realities present in an actual DWDS means that any Pb(II) solubility model is best applied to understand trends in concentration with changing water quality (i.e., qualitative) rather than

simulating actual TOTSOLPb levels (i.e., quantitative). Major Pb(II) solubility model limitations associated with assumptions made in the Pb(II) solubility model are summarized in Table 3. These limitations provide reasons to explain cases where theoretical model simulations based on measured water quality inputs do not correspond with measured TOTSOLPb concentrations.

**TABLE 3** Lead(II) solubility model limitations summary

Model assumptions <sup>a</sup>	Reality in actual drinking water distribution systems
Equilibrium always exists	<ul style="list-style-type: none"> <li>Additional processes impacting lead release may provide kinetic limitations such that equilibrium is never obtained, including rates of               <ul style="list-style-type: none"> <li>Corrosion</li> <li>Scale formation</li> <li>Scale dissolution</li> <li>Solid interconversions</li> </ul> </li> </ul>
Mass transfer ignored	<ul style="list-style-type: none"> <li>Diffusion limitations exist               <ul style="list-style-type: none"> <li>Within pipe scale and will be dependent on scale structure</li> <li>Between the pipe scale surface and bulk water and will be dependent on system hydraulics</li> </ul> </li> </ul>
Solid/scale <ul style="list-style-type: none"> <li>Single solid controls solubility</li> <li>Lead(II) only</li> </ul>	<ul style="list-style-type: none"> <li>Scales are commonly mixtures of multiple solids</li> <li>Equilibrium constants               <ul style="list-style-type: none"> <li>Multiple estimates may exist for a given solid</li> <li>May not be known for solids present</li> </ul> </li> <li>Lead(IV) solids may exist</li> </ul>
Soluble lead only	<ul style="list-style-type: none"> <li>Particle lead may be present and included in lead samples</li> </ul>
25°C temperature	<ul style="list-style-type: none"> <li>Temperatures vary and every equilibrium constant (Tables 1 and 2) is dependent on temperature</li> </ul>
No biofilm or NOM interactions	<ul style="list-style-type: none"> <li>Biofilm and NOM will be present and may impact lead release</li> </ul>
Phosphates <ul style="list-style-type: none"> <li>No scavenging</li> <li>Orthophosphate only</li> </ul>	<ul style="list-style-type: none"> <li>Scavenging may occur through complexation and/or precipitation (e.g., calcium)</li> <li>Polyphosphates may be present and introduce impacts not included in the solubility model               <ul style="list-style-type: none"> <li>Unknown complexes</li> <li>Interference with formation of crystalline lead(II) carbonate or orthophosphate solids</li> </ul> </li> </ul>

Abbreviations: NOM, natural organic matter.

<sup>a</sup>Model assumes that a solubility relationship controls the level of dissolved chemical in the water and uses the provided equilibrium water chemistry to simulate potential solid formation and resulting dissolved chemical species concentrations, but no assumptions are made with regards to the underlying corrosion (e.g., galvanic or uniform) or metals release mechanisms or rates.



Specifically, comparing solubility model simulated TOTSOLPb concentrations (e.g., TELSS, LEADSOL, or other solubility model output) to measured TOTSOLPb concentrations from drinking water tap samples is inappropriate because the simulated TOTSOLPb concentration is predicated on direct contact with a Pb(II) solid (Triantafyllidou et al., 2021).

To illustrate the potential impact of the limitations (Table 3), one of the limitations was directly assessed with the TELSS code. Figure 1 illustrates how theoretical simulated TOTSOLPb concentrations change based on using two different published values for a given equilibrium constant: (i) the default equilibrium constant for hydroxypyromorphite in the TELSS code (Table 1,  $\log K = -62.83$ ) or (ii) the alternate value (Table 2,  $\log K = -66.77$ ). The simulated TOTSOLPb concentration decreased 84% when using the alternative value for the equilibrium constant, but it should be noted that the same trends with DIC and pH are still seen in both the simulated TOTSOLPb concentrations (Figure 1).

### 3 | PRACTICAL RELATIONSHIPS

Pb(II) solubility diagrams have been used widely over the years in the drinking water field (e.g., American Water Works

Association, 2017; Brandhuber, 2020; Edwards et al., 1999; Schock, 1989), many of which have been reproduced from the original efforts of Schock (Schock, 1980, 1981; Schock et al., 1996) who created Pb(II) solubility diagrams using output from the LEADSOL model implemented in Fortran. These developed Pb(II) solubility diagrams illustrated important theoretical relationships regarding pH, DIC, and/or orthophosphate and have informed guidance related to corrosion control (United States Environmental Protection Agency, 2019), but LEADSOL is not easily shareable today and requires the user to have some understanding of running Fortran code. To illustrate use of the TELSS code to overcome these limitations, TOTSOLPb concentrations were simulated under various scenarios to illustrate several practical relationships with regard to TOTSOLPb concentrations.

#### 3.1 | Impact of DIC, pH, and dissolved species on simulated TOTSOLPb concentrations

Based on Schock (1980, 1981) and originally presented by Schock and Lytle (2011), Figure 2 illustrates the relationship among DIC concentrations, pH, and TOTSOLPb concentrations. A DIC increase below a pH of approximately 7.5 decreases TOTSOLPb concentrations, but a DIC increase above pH 8 tends to increase TOTSOLPb concentrations until near pH 10 where a local maximum

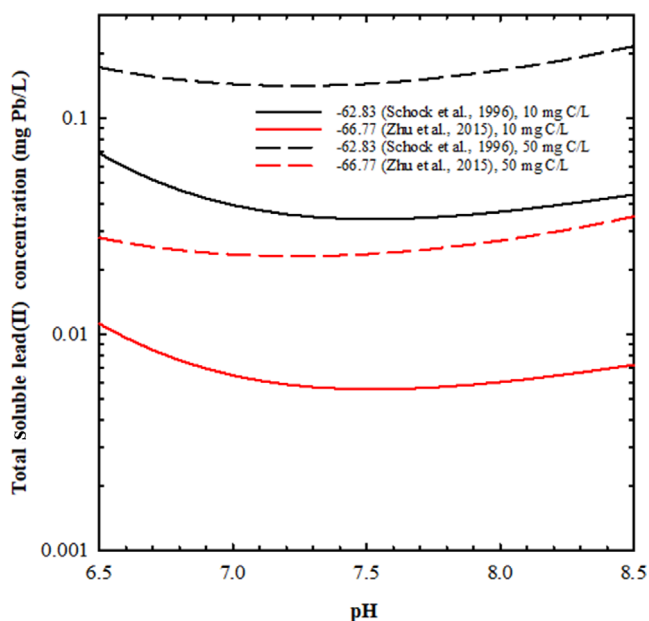


**FIGURE 1** Impact on simulated total soluble lead(II) (TOTSOLPb) concentrations when using different equilibrium constant values for hydroxypyromorphite,  $\text{Pb}_5(\text{PO}_4)_3\text{OH}$ , solubility (Tables 1 and 2) and assuming hydroxypyromorphite is the controlling lead(II) solid (5 mM ionic strength; 1 mg  $\text{PO}_4/\text{L}$  orthophosphate)

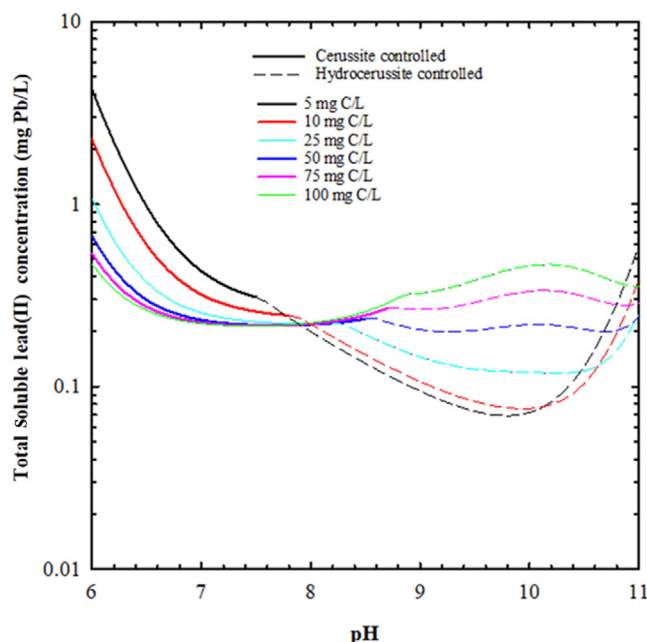


**FIGURE 2** Impact of pH and dissolved inorganic carbon (DIC) concentration on simulated total soluble lead(II) (TOTSOLPb) concentration (5 mM ionic strength). Controlling lead(II) solid is denoted by linetype

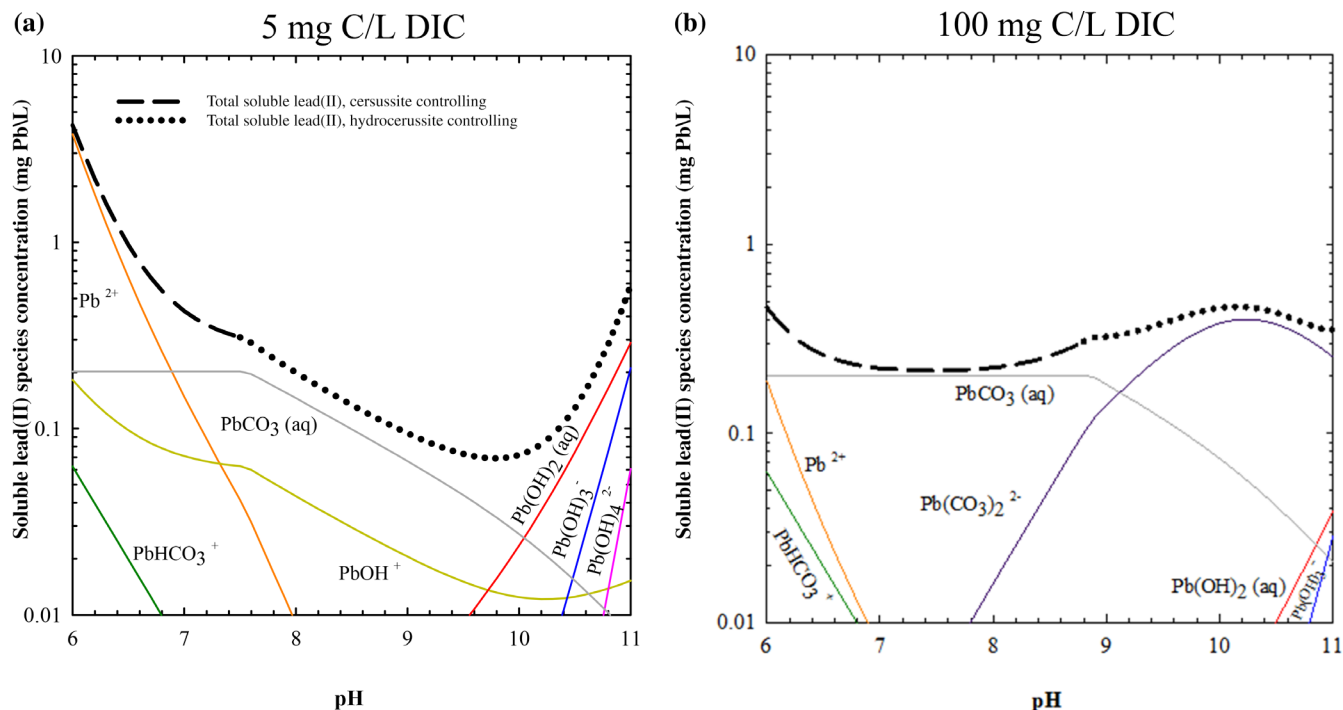


**FIGURE 3** Impact of pH and dissolved inorganic carbon (DIC) concentrations on simulated soluble lead(II) ion ( $\text{Pb}^{2+}$ ), soluble lead(II) complexes, and total soluble lead(II) (TOTSOLPb) concentrations (5 mM ionic strength). The controlling lead(II) solid for TOTSOLPb switches from cerussite to hydrocerussite above pH 7.5 and 8.8 in panels (a) and (b), respectively (denoted by TOTSOLPb linetype). Legend in panel (a) applies to both panels. Note that most TOTSOLPb is present in lead(II) complexes with little  $\text{Pb}^{2+}$  present, except in panel (a) for pH less than 7

is reached for TOTSOLPb concentrations. Around pH 8, DIC changes are simulated to have minor impacts on TOTSOLPb concentrations. As pH increases from pH 6 to 11, the predicted controlling carbonate solid shifts from cerussite,  $\text{PbCO}_3$  (s), to hydrocerussite,  $\text{Pb}_3(\text{CO}_3)_2(\text{OH})_2$  (s). The pH of the transition is dependent on DIC concentration and increases from occurring above a pH of 7.5 to above a pH of 8.8 for simulations with 5 and 100 mg C/L DIC concentrations, respectively. It is also noteworthy that there is a zone of pH from the high 7 s to low 8 s in which changes in DIC have a relatively small impact on simulated TOTSOLPb solubility, which accounts for some of the early skepticism that DIC mattered in Pb release control from the results of utility corrosion pilot studies. Conversely, for  $\geq 25$  mg C/L DIC, pH plays a relatively small role between pHs 7.5 and 8.3.

TELSS code also provides the concentrations of individual Pb(II) species ( $\text{Pb}^{2+}$  and aqueous Pb(II) complexes), which are necessary to understand TOTSOLPb concentration trends (Figure 2). For example, solubility diagrams for water containing 5 and 100 mg C/L DIC have been generated to illustrate the distribution of aqueous Pb(II) species across a wide pH range (Figure 3). In 5 mg C/L DIC water (Figure 3a), as pH increases from 6 to 11, the TOTSOLPb concentration is dominated by  $\text{Pb}^{2+}$  from pH 6 to 7, whereas the neutral  $\text{PbCO}_3$  (aq) complex dominates from pH 7 to

10, and the neutral  $\text{Pb}(\text{OH})_2$  (aq) complex dominates from pH 10 to 11. Increasing the DIC to 100 mg C/L (Figure 3b) shifts the dominance of the Pb(II) carbonate complexes in the distribution of TOTSOLPb species to cover the entire pH range of 6–11 and illustrates how increasing DIC increases TOTSOLPb concentration (Figure 2). From pH 6 to approximately pH 9, neutral  $\text{PbCO}_3$  (aq) dominates TOTSOLPb concentration. At approximately pH 9,  $\text{PbCO}_3$  (aq) and  $\text{Pb}(\text{CO}_3)_2^{2-}$  are equally present, and above pH 9,  $\text{Pb}(\text{CO}_3)_2^{2-}$  dominates TOTSOLPb concentration.

The examination of Pb(II) speciation diagrams (Figure 3) helps explain Pb mineral transitions and TOTSOLPb concentration trends. For example, the minimum TOTSOLPb concentration in 5 mg C/L DIC water is simulated to be at pH 10 where both  $\text{PbCO}_3$  (aq) and  $\text{Pb}(\text{OH})_2$  (aq) dominate TOTSOLPb concentration, but at 100 mg C/L DIC, the  $\text{Pb}(\text{CO}_3)_2^{2-}$  complex dominates TOTSOLPb concentration at pH 10 and, as a result, increases TOTSOLPb concentration. In addition, the pH of minimum TOTSOLPb concentration shifts from pH 10 to pH 7.5. In either DIC case,  $\text{PbCO}_3$  (aq) concentration starts decreasing once the controlling Pb(II) solid transitions from cerussite to hydrocerussite (above pH 7.5 for 5 mg C/L DIC; above pH 8.8 for 100 mg C/L DIC).

### 3.2 | Effects of DIC and orthophosphate concentrations on simulated TOTSOLPb concentrations

Orthophosphate addition is one possible option for a water system to reduce TOTSOLPb concentrations. The theoretical impact of orthophosphate concentration on TOTSOLPb concentrations depends on both the DIC concentration and pH of the water. As shown in Figure 4 (see also Figure S12), when orthophosphate is present,

TOTSOLPb concentrations increase as DIC concentrations increase until the TOTSOLPb concentration reaches the same concentration as when no orthophosphate is present (i.e., up until the controlling Pb(II) solid changes from a phosphate-containing solid to a carbonate-containing solid). In the region of the solubility diagram where a phosphate solid controls solubility (colored portion of lines in Figure 4), the TOTSOLPb concentration decreases as orthophosphate concentration increases, but as the DIC concentration further increases to where a

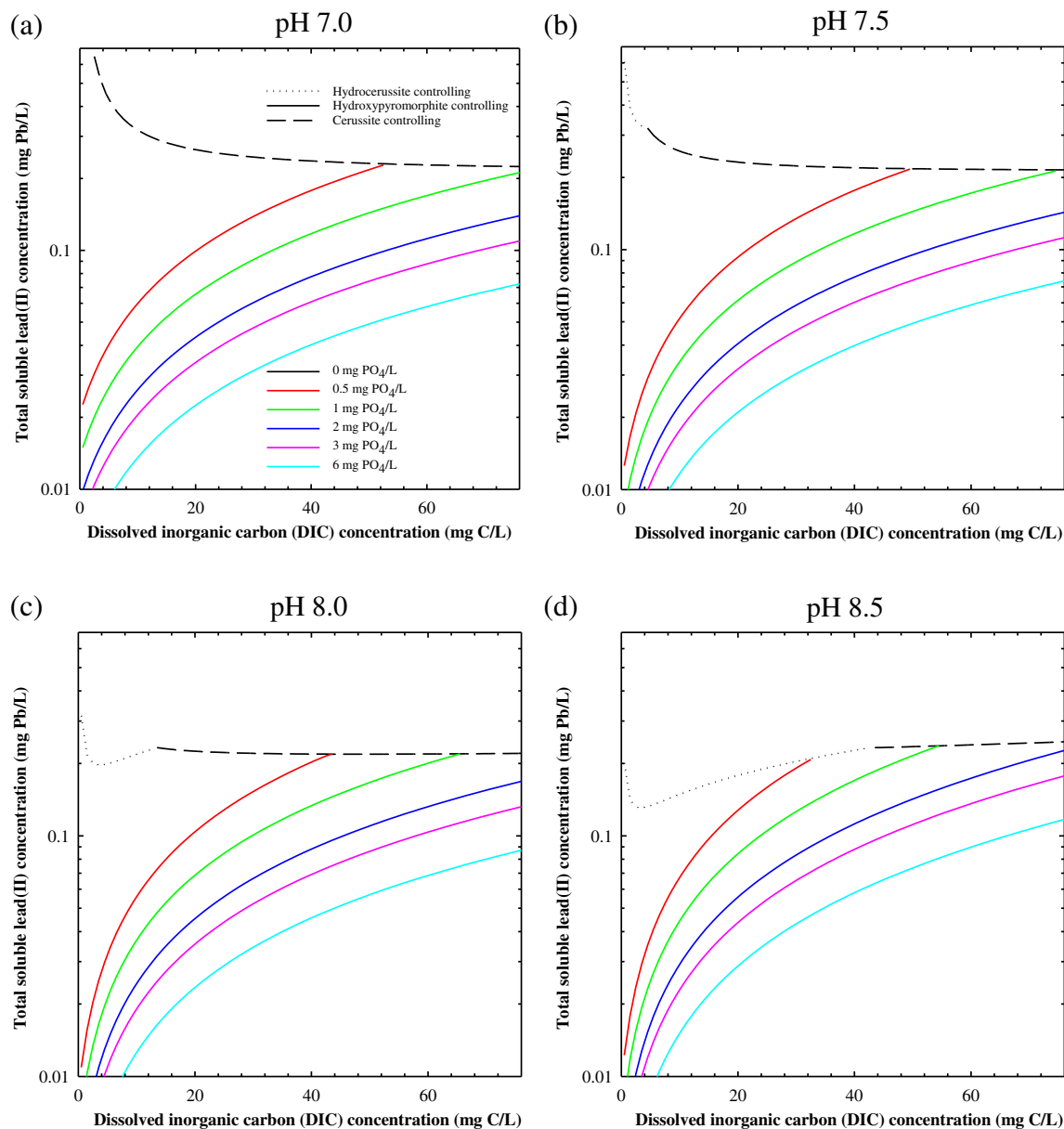


**FIGURE 4** Impact of dissolved inorganic carbon (DIC) and orthophosphate concentrations on simulated total soluble lead(II) (TOTSOLPb) concentrations for several pHs (pH: 7.0 (a), 7.5 (b), 8.0, (c), and 8.5 (d); 5 mM ionic strength; cerussite, hydrocerussite, and hydroxypyromorphite solids considered for controlling solubility). TOTSOLPb is presented on a logarithmic scale (see Figure S12 for a linear scale version). Legend in panel (a) applies to all panels, and linetype denotes controlling lead(II) solid. For simulations with orthophosphate present and as DIC increases, the simulations proceed on the 0 mg  $\text{PO}_4/\text{L}$  line once connected (i.e., as if orthophosphate had not been added)



carbonate solid controls solubility, the TOTSOLPb concentration is as though there is no orthophosphate present (i.e., black lines in Figure 4). Overall, Figure 4 illustrates that at typical drinking water pHs and for the solids and solubility constants considered, orthophosphate should provide some advantage in reducing TOTSOLPb solubility as hydroxypyromorphite is the controlling Pb(II) solid versus hydrocerussite or cerussite.

The minimum TOTSOLPb concentration for each given DIC and orthophosphate concentration occurs around a pH of 7.5, which is readily apparent in Figure 5 (see also Figure S13). Figure 6 illustrates the diminishing returns associated with orthophosphate concentration (0.05–6 mg PO<sub>4</sub>/L orthophosphate) as DIC concentration increases. For a given orthophosphate concentration, the resulting decrease in simulated TOTSOLPb concentration

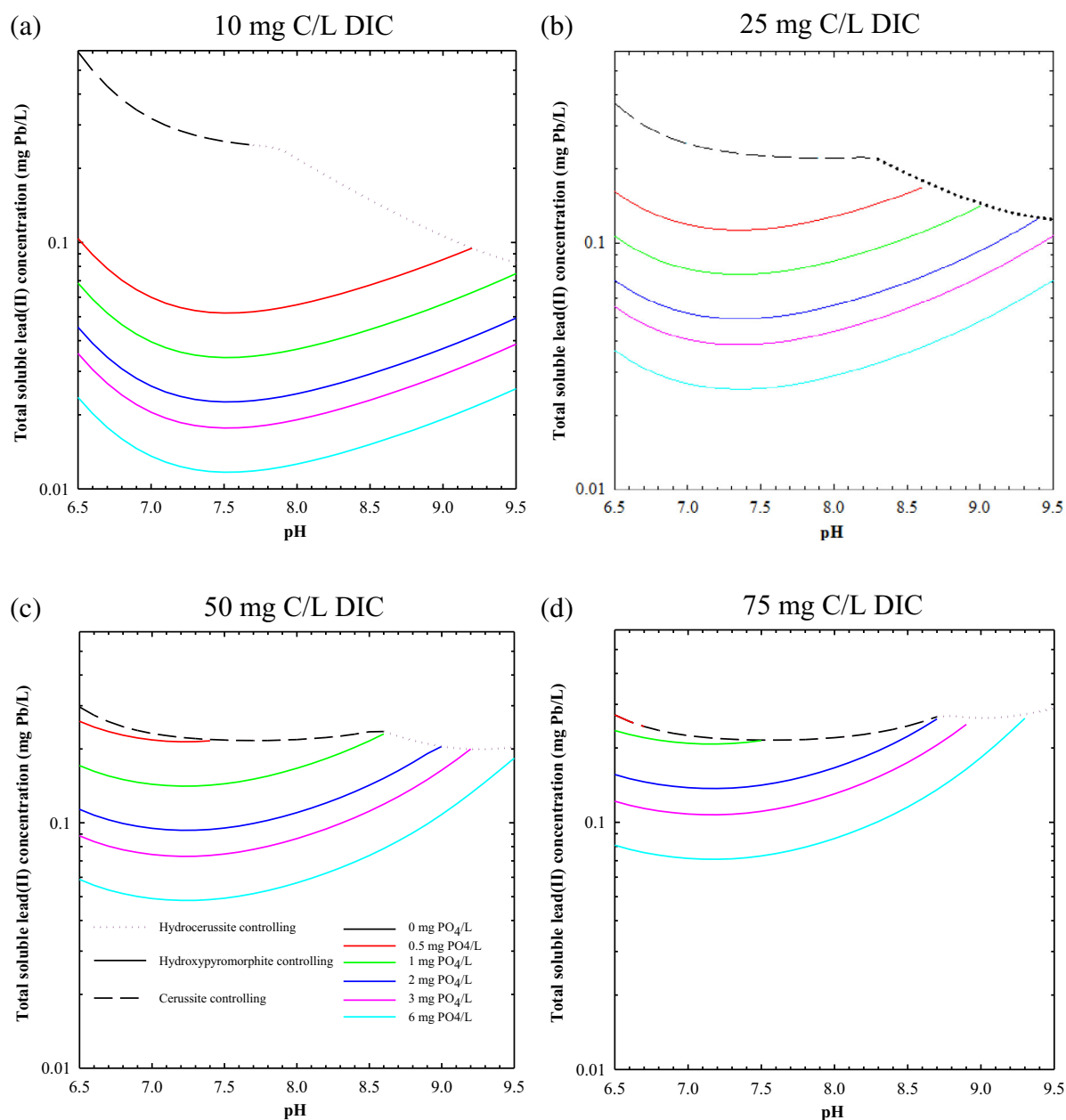


**FIGURE 5** Impact of pH and orthophosphate concentrations on simulated total soluble lead(II) (TOTSOLPb) concentrations for several dissolved inorganic carbon (DIC) concentrations (DIC (mg C/L): 10 (a), 25 (b), 50, (c), and 75 (d); 5 mM ionic strength; cerussite, hydrocerussite, and hydroxypyromorphite solids considered for controlling solubility). TOTSOLPb is presented on a logarithmic scale (see Figure S13 for a linear scale version). Legend in panel (c) applies to all panels, and linetype denotes controlling lead(II) solid. For simulations with orthophosphate present and as pH increases, these simulations proceed on the 0 mg PO<sub>4</sub>/L line once connected (i.e., as if orthophosphate had not been added)

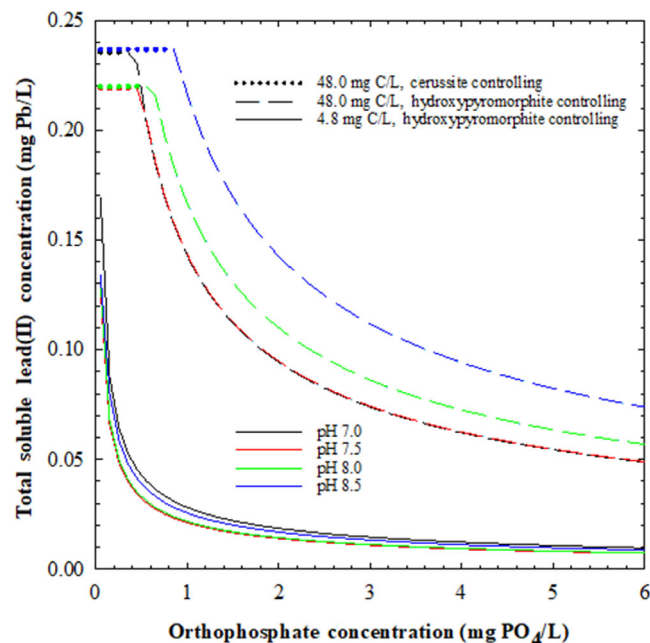


**FIGURE 6** Impact of pH and orthophosphate concentrations (0.05–6 mg PO<sub>4</sub>/L orthophosphate) on simulated total soluble lead(II) (TOTSOLPb) concentrations for a low (4.8 mg C/L) and high (48 mg C/L) dissolved inorganic carbon (DIC) concentration (10 mM ionic strength; cerussite, hydrocerussite, and hydroxypyromorphite solids considered for controlling solubility). The controlling lead(II) solid is denoted by linetype, except for a single simulation point (4.8 mg C/L DIC, 0.05 mg PO<sub>4</sub>/L orthophosphate, and pH 8.5) where the controlling lead(II) solid is hydrocerussite

is more pronounced as DIC concentration decreases. This indicates that as DIC concentration increases, it is expected that greater and greater orthophosphate concentrations would be required to achieve the same impact seen at lower DIC concentrations. In fact, greater doses of orthophosphate (e.g., 4–6 mg PO<sub>4</sub>/L) have been required to achieve TOTSOLPb under 0.010 mg/L (Cardew, 2008; Hayes et al., 2008). Overall, the simulations and literature support that a priori no single dose of orthophosphate is expected applicable to all drinking water systems to achieve a target TOTSOLPb concentration; therefore, system-specific water chemistry needs to be considered to prevent over or under-dosing orthophosphate.

### 3.3 | Impact of chloride and sulfate concentrations on simulated TOTSOLPb concentrations in low pH water

An important relationship that can be investigated using a Pb(II) solubility model is the theoretical impacts of chloride and sulfate concentrations on TOTSOLPb concentrations

that can become important where galvanic corrosion is occurring at Pb-brass or Pb-copper connections (Clark et al., 2013; DeSantis et al., 2018; Doré et al., 2019; Nguyen et al., 2011). During galvanic corrosion involving Pb, the pH where Pb will be released (i.e., at the anode) will be low (e.g., pH < 6) because of hydrolysis reactions and potentially much lower than the bulk water pH because of mass transfer limitations (Ma et al., 2018, 2019). For water with a pH < 6, at low ionic strength, and depending on the DIC concentration, anglesite (PbSO<sub>4</sub> (s)) is the theoretical Pb(II) solid controlling solubility, and anglesite solubility is driven primarily by sulfate concentration (Figure 7). In the absence of sulfate, laurionite (PbClOH (s)) is the theoretical solid controlling solubility for water with otherwise similar conditions. Anglesite and laurionite, to a much lesser extent, have been found at joints removed from drinking water systems where indications of galvanic corrosion were present (DeSantis et al., 2018), supporting their formation in actual DWDSs and their role in solubility control in localized microenvironments.

If anglesite is controlling Pb(II) solubility (i.e., the nearly horizontal regions in Figure 7), then an approximate equation for TOTSOLPb concentrations can be derived from Equations (4) to (6), resulting in Equation (7). In Equations (4) through (7), { } indicates activity, [ ] indicates concentration (moles/L), and equilibrium constants correspond to those presented in Table 1.

$$K_{\text{solid}} = 10^{-7.79} = \frac{\{\text{Pb}^{2+}\}\{\text{SO}_4^{2-}\}}{\{\text{PbSO}_{4(s)}\}} \approx [\text{Pb}^{2+}][\text{SO}_4^{2-}] \quad (4)$$

$$K_{1,\text{SO}_4} = 10^{2.73} = \frac{\{\text{PbSO}_{4(\text{aq})}\}}{\{\text{Pb}^{2+}\}\{\text{SO}_4^{2-}\}} \approx \frac{[\text{PbSO}_{4(\text{aq})}]}{[\text{Pb}^{2+}][\text{SO}_4^{2-}]} \quad (5)$$

$$K_{1,\text{Cl}} = 10^{1.59} = \frac{\{\text{PbCl}^+\}}{\{\text{Pb}^{2+}\}\{\text{Cl}^-\}} \approx \frac{[\text{PbCl}^+]}{[\text{Pb}^{2+}][\text{Cl}^-]} \quad (6)$$

$$[\text{TOTSOLPb}] \approx \frac{K_{\text{solid}}}{[\text{SO}_4^{2-}]} + K_{\text{solid}}K_{1,\text{SO}_4} + K_{\text{solid}}K_{1,\text{Cl}} \frac{[\text{Cl}^-]}{[\text{SO}_4^{2-}]} \quad (7)$$

The last term in Equation (7) illustrates the impact of the chloride to sulfate ratio on the simulated TOTSOLPb concentration and is often cited as an important parameter for Pb release from galvanic junctions (Edwards & Triantafyllidou, 2007; Nguyen et al., 2011). It is also noted that from a purely theoretical Pb(II) solubility view and based on the first term in Equation (7), sulfate concentration alone may impact TOTSOLPb concentration and is simulated to decrease the TOTSOLPb concentration as sulfate concentration increases if the chloride to

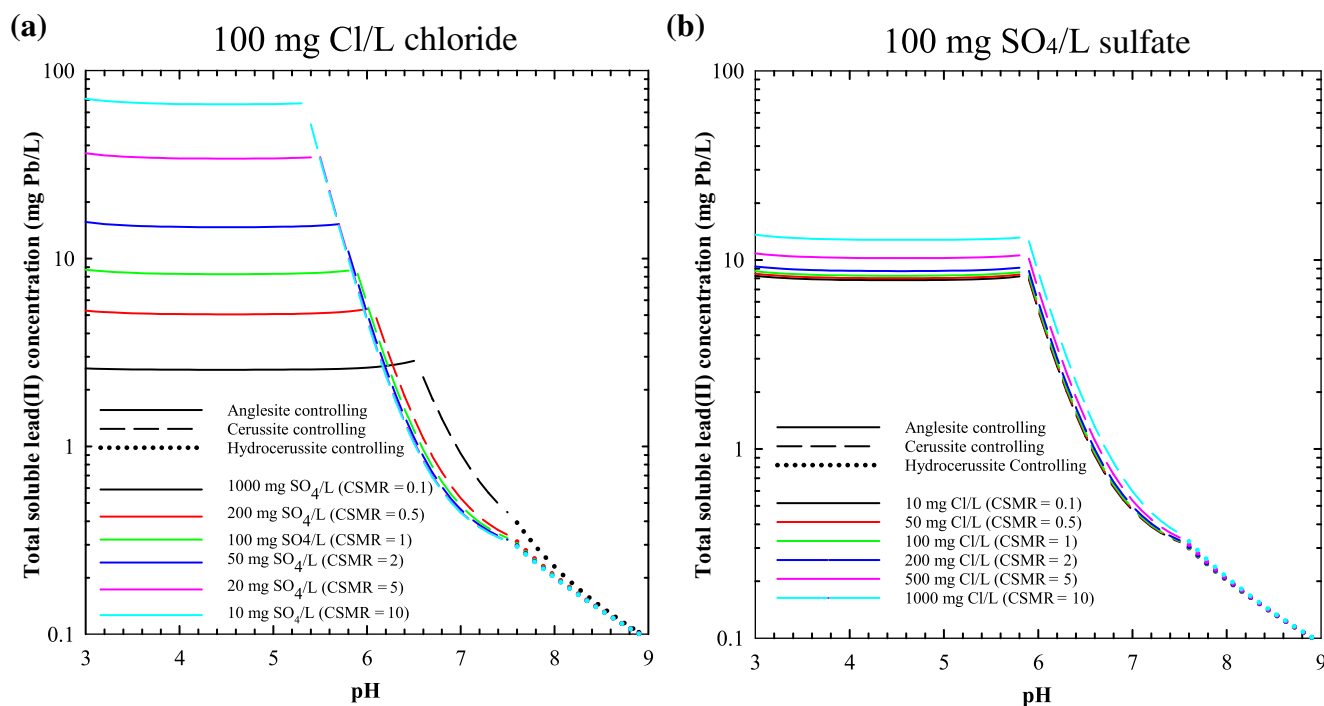


**FIGURE 7** Impact of chloride and sulfate concentrations on simulated total soluble lead(II) (TOTSOLPb) concentrations (5 mM ionic strength; 5 mg C/L dissolved inorganic carbon (DIC) concentration) for (a) holding chloride constant and varying sulfate concentration and (b) holding sulfate constant and varying chloride concentration. Controlling lead(II) solid transitions as pH increases from 3 to 9 and is denoted by linetype: (i) anglesite controls in the horizontal region from pH 3 to approximately pH 5.5 to 6.5, (ii) cerussite then controls to approximately pH 7.5, (iii) and hydrocerussite then controls to pH 9. CSMR = chloride to sulfate mass ratio

sulfate ratio remains constant, an expected result as the controlling Pb(II) solid contains sulfate. Furthermore, as the species involved in Equation (7) vary minimally at pHs greater than 3, TOTSOLPb concentration is essentially not dependent on pH if anglesite is the controlling Pb(II) solid (Figure 7). A final observation on Equation (7) is that the middle term ( $K_{\text{solid}}K_{1,\text{SO}_4}$ ) is a constant ( $10^{-5.06}$ ), resulting from the neutral  $\text{PbSO}_4$  (aq) complex; therefore, with anglesite as the controlling Pb(II) solid, there is a theoretical minimum TOTSOLPb concentration (1.8 mg/L) that can be obtained locally at the microenvironment.

The DIC concentration impact can best be viewed by looking at how the Pb(II) carbonate complexes impact TOTSOLPb concentrations at these lower pHs. For example, Pb(II) carbonate complexes in the anglesite controlling solubility region have an insignificant impact on TOTSOLPb concentrations (Figure 8), however, an increase in DIC concentration lowers the pH where the controlling Pb(II) solid transitions between anglesite and cerussite (Figure 8). The pH at which the transition between anglesite and cerussite occurs is also impacted by sulfate concentration; increasing the total sulfate concentration from 10 to 1000 mg SO<sub>4</sub>/L increases the transition pH from 5.3 to 6.5 (Figure 7a). TOTSOLPb concentrations in the anglesite controlling region are controlled predominantly by sulfate according to

Equation (7) (Figure 7a) because the Pb(II) solid contains sulfate and the presence of an important Pb(II) sulfate complex (e.g.,  $\text{PbSO}_4$  (aq)). For example, decreasing the sulfate concentration from 100 to 50 mg SO<sub>4</sub>/L when the chloride concentration is constant at 100 mg Cl/L (a resultant increase in the chloride to sulfate mass ratio [CSMR] from 1 to 2) increases the simulated TOTSOLPb concentration by about 78% (Figure 7a).

The role of chloride on TOTSOLPb concentration in this pH region is also important because of the presence of a Pb(II) chloride complex ( $\text{PbCl}^+$ ) but at a much lesser extent than sulfate. For example, increasing the chloride concentration from 100 to 200 mg Cl/L while the concentration of sulfate is constant at 100 mg SO<sub>4</sub>/L (a resultant increase in the CSMR from 1 to 2) only increases the TOTSOLPb concentration by approximately 6% (Figure 7b). Although the bulk water pH in any typical DWDS is above 6.5, pH values as low as 3 and the formation of anglesite have been observed in microenvironments where Pb is galvanically connected to copper or brass (DeSantis et al., 2018; Ma et al., 2019).

Such analyses have potentially important practical implications for Pb release with some limitations. First, it is not clear what the concentrations of sulfate and chloride are locally at galvanic connections (relative to bulk

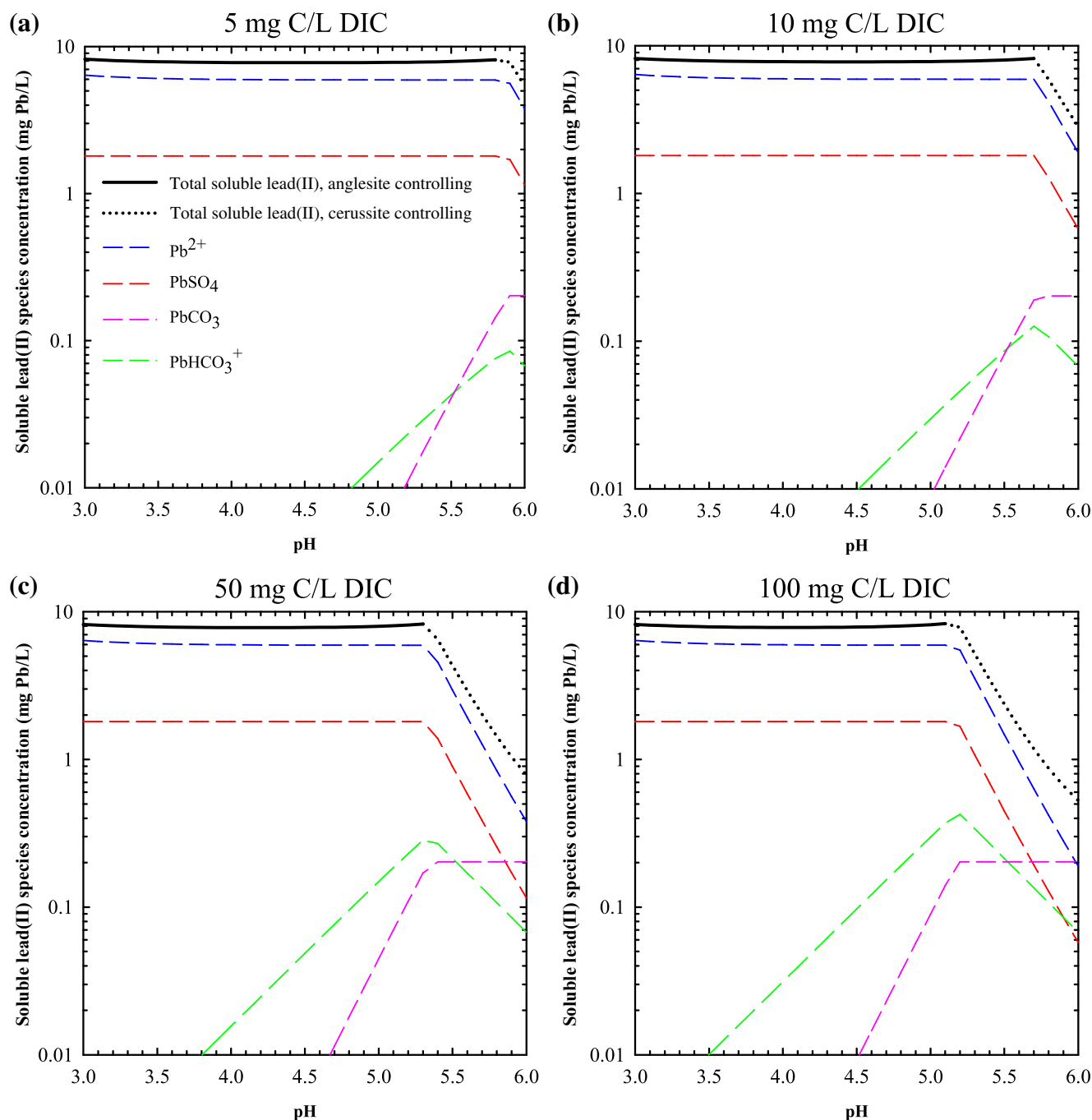


**FIGURE 8** Impact of dissolved inorganic carbon (DIC) concentration on simulated lead(II) ion ( $\text{Pb}^{2+}$ ), major lead(II) carbonate complexes, and total soluble lead(II) (TOTSOLPb) concentrations (DIC (mg C/L): 5 (a), 10 (b), 50 (c), and 100 (d); 5 mM ionic strength; 100 mg  $\text{SO}_4/\text{L}$  sulfate). Legend in panel (a) applies to all panels, and the controlling lead(II) solid is denoted by the TOTSOLPb linetype

water) where presumably the pH is acidic and an abundance of metal cations attract and concentrate anions. Second, it is not clear to what extent local changes in anglesite solubility have on bulk water TOTSOLPb (e.g., mass transfer limitations, hydraulics, and corrosion kinetics may limit impacts to bulk water Pb concentrations). Nonetheless, the model provides a useful tool to analyze hypothetical local condition scenarios and establishes a framework for understanding the roles of sulfate

and chloride (and CSMR) in these local environments. For TOTSOLPb concentrations (i.e., equilibrium consideration), sulfate is simulated to be more impactful as it is required for anglesite formation whereas chloride is far less important, but chloride may impact the rate (i.e., kinetic consideration) of galvanic corrosion that is not captured by equilibrium solubility models (see Table 3) (Ng & Lin, 2016; Nguyen et al., 2011; Schock & Lytle, 2011).

## 4 | SUMMARY

The developed TELSS code is freely available for download and can be used to simulate theoretical equilibrium TOTSOLPb concentrations, using user-selected water quality conditions. Using the TELSS code, several practical relationships regarding TOTSOLPb concentration trends have been highlighted, including the varied impact of DIC concentration and pH when orthophosphate is not present, the beneficial impact of orthophosphate and associated DIC concentration and pH impacts when simple Pb(II) carbonates and phosphate scales form, and the potential impact of sulfate and chloride concentrations at low pH when the controlling Pb(II) solid is anglesite. The TELSS code provides a tool to allow drinking water practitioners to simulate TOTSOLPb concentrations for their specific water quality without relying on implementing a model on their own or inferring trends based on solubility diagrams presented in the literature that may not match their exact conditions of interest. The TELSS code provides a standardized and accessible model to verify model implementations in additional environments, may be expanded and updated by the end-user to meet their specific needs, and provides an example of how to generally create a theoretical solubility model in an open source format that could be applied to other scenarios of interest in drinking water or other disciplines (e.g., copper (II) solubility model).

## ACKNOWLEDGMENTS

This work has been subjected to the United States Environmental Protection Agency's (Agency's) review and has been approved for publication. The views expressed in this manuscript are those of the author and do not necessarily represent the views or policies of the Agency. Any mention of trade names, products, or services does not imply an endorsement by the Agency. The Agency does not endorse any commercial products, services, or enterprises.

## CONFLICT OF INTEREST

The authors have no conflict of interest to declare.


## AUTHOR CONTRIBUTIONS

**David G. Wahman:** Writing – original draft. **Matthew D. Pinelli:** Writing – original draft. **Michael R. Schock:** Writing – original draft. **Darren A. Lytle:** Writing – original draft.


## DATA AVAILABILITY STATEMENT

The data that support the findings of this study are openly available at <http://doi.org/10.23719/1520732>

## ORCID

David G. Wahman  <https://orcid.org/0000-0002-0167-8468>

Matthew D. Pinelli  <https://orcid.org/0000-0003-1325-8206>

Michael R. Schock  <https://orcid.org/0000-0001-9248-6690>

Darren A. Lytle  <https://orcid.org/0000-0002-5282-4541>

## REFERENCES

- American Water Works Association. (2017). *Internal corrosion control in water distribution systems (AWWA manual M58)* (2nd ed.). American Water Works Association.
- Benjamin, M. M. (2002). *Water chemistry* (1st ed.). McGraw-Hill.
- Bethke, C. M. (2010). *Geochemical and biogeochemical reaction modeling* (2nd ed.). Cambridge University Press.
- Brandhuber, P. (2020). *Overview of lead corrosion control*, LCR revisions and corrosion control basics, Webinar, February 5, 2020; American Water Works Association.
- Brown, R. A., McTigue, N. E., & Cornwell, D. A. (2013). Strategies for assessing optimized corrosion control treatment of lead and copper. *Journal American Water Works Association*, 105(5), 62.
- Cardew, P. T. (2008). Measuring the benefit of orthophosphate treatment on lead in drinking water. *Journal of Water and Health*, 7(1), 123.
- Chang, W., Cheng, J., Allaire, J., Xie, Y. & Mc Pherson, J. (2020). Shiny: Web application framework for R. R package version 1.5.0.
- Clark, B., Cartier, C., St Clair, J., Triantafyllidou, S., Prevost, M., & Edwards, M. (2013). Effect of connection type on galvanic corrosion between Lead and copper pipes. *Journal American Water Works Association*, 105(10), 69.
- Crouch, S. R., & Holler, F. J. (2014). *Applications of Microsoft Excel in analytical chemistry* (2nd ed.). Brooks/Cole, Cengage Learning.
- Del Toral, M. A., Porter, A., & Schock, M. R. (2013). Detection and evaluation of elevated Lead release from service lines: A field study. *Environmental Science & Technology*, 47(16), 9300.
- DeSantis, M. K., Triantafyllidou, S., Schock, M. R., & Lytle, D. A. (2018). Mineralogical evidence of galvanic corrosion in drinking water Lead pipe joints. *Environmental Science & Technology*, 52(6), 3365.
- Doddrill, D. M., & Edwards, M. (1995). Corrosion control on the basis of utility experience. *Journal American Water Works Association*, 87(7), 74.
- Doré, E., Deshommes, E., Laroche, L., Nour, S., & Prévost, M. (2019). Study of the long-term impacts of treatments on lead release from full and partially replaced harvested lead service lines. *Water Research*, 149, 566–577.
- Economic and Engineering Services. (1990). *Lead control strategies (report #90559)*. American Water Works Association Research Foundation and American Water Works Association.
- Edwards, M., Jacobs, S., & Doddrill, D. (1999). Desktop guidance for mitigating Pb and Cu corrosion by-products. *Journal American Water Works Association*, 91(5), 66.
- Edwards, M., & Triantafyllidou, S. (2007). Chloride-to-sulfate mass ratio and lead leaching to water. *Journal American Water Works Association*, 99(7), 96.



- Federal Register. (1991a). Drinking water regulations; maximum contaminant level goals and national primary drinking water regulations for lead and copper, final rule; Correction, 56:135:32112.
- Federal Register. (1991b). Maximum contaminant level goals and national primary drinking water regulations for lead and copper, final rule, 56:110:26460.
- Federal Register. (1992). Drinking water regulations: Maximum contaminant level goals and national primary drinking water regulations for lead and copper, final rule; correcting amendments, 57:125:28785.
- Gustaffson, J. P. (2015). *Visual MINTEQ version 3.1*. KTH.
- Hayes, C. R., Incledon, S., & Balch, M. (2008). Experience in Wales (UK) of the optimisation of ortho-phosphate dosing for controlling lead in drinking water. *Journal of Water and Health*, 6(2), 177.
- Hunt, D. T. E., & Creasey, J. D. (1980). *Calculation of equilibrium trace metal speciation and solubility in aqueous systems by a computer method, with particular reference to Lead, technical report TR-151*. Water Research Centre.
- Jackson, P. J., & Sheiham, I. (1980). *Calculation of Lead solubility in water, technical report TR-152*. Water Research Centre.
- Jurgens, B. C., Parkhurst, D. L., & Belitz, K. (2019). Assessing the Lead solubility potential of untreated groundwater of the United States. *Environmental Science & Technology*, 53(6), 3095.
- Kirmeyer, G. J., Sandvig, A. M., Pierson, G. L., & Neff, C. H. (1994). *Development of a pipe loop protocol for lead control*. American Water Works Association Research Foundation and American Water Works Association.
- Lothenbach, B., Ochs, M., Wanner, H., & Yui, M. (1999). *Thermodynamic data for the speciation and solubility of Pd, Pb, Sn, Sb, Nb and Bi in aqueous solution*. Japan Nuclear Cycle Development Institute.
- Ma, X. M., Armas, S. M., Soliman, M., Lytle, D. A., Chumbimuni-Torres, K., Tetard, L., & Lee, W. H. (2018). In situ monitoring of  $Pb^{2+}$  leaching from the galvanic joint surface in a prepared chlorinated drinking water. *Environmental Science & Technology*, 52(4), 2126.
- Ma, X. M., Lytle, D. A., & Lee, W. H. (2019). Microelectrode investigation on the corrosion initiation at lead-brass galvanic interfaces in chlorinated drinking water. *Langmuir*, 35(40), 12947.
- Malmberg, C. G., & Maryott, A. A. (1956). Dielectric constant of water from 0° to 100° C. *Journal of Research of the National Bureau of Standards*, 56(1), 1.
- Nasanen, R., & Lindell, E. (1976). Studies on Lead(II) hydroxide salts. Part I. the solubility product of  $Pb(OH)Cl$ . *Finnish Chemical Letters*, 95–98.
- Ng, D.-Q., & Lin, Y.-P. (2016). Effects of pH value, chloride and sulfate concentrations on galvanic corrosion between Lead and copper in drinking water. *Environmental Chemistry*, 13(4), 602.
- Nguyen, C. K., Stone, K. R., & Edwards, M. A. (2011). Chloride-to-sulfate mass ratio: Practical studies in galvanic corrosion of Lead solder. *Journal American Water Works Association*, 103(1), 81.
- Powell, K. J., Brown, P. L., Byrne, R. H., Gajda, T., Hefter, G., Leuz, A. K., Sjöberg, S., & Wanner, H. (2009). Chemical speciation of environmentally significant metals with inorganic ligands—Part 3: The  $Pb^{2+}$ ,  $OH^-$ ,  $Cl^-$ ,  $CO_3^{2-}$ ,  $SO_4^{2-}$ , and  $PO_4^{3-}$  systems—IUPAC technical report). *Pure and Applied Chemistry*, 81(12), 2425.
- Powell, K. J., Brown, P. L., Byrne, R. H., Gajda, T., Hefter, G., Sjöberg, S., & Wanner, H. (2005). Chemical speciation of environmentally significant heavy metals with inorganic ligands—Part 1: The  $Hg^{2+}$ ,  $Cl^-$ ,  $OH^-$ ,  $CO_3^{2-}$ ,  $SO_4^{2-}$ , and  $PO_4^{3-}$  aqueous systems—IUPAC technical report). *Pure and Applied Chemistry*, 77(4), 739.
- R Core Team. (2020). *R: A language and environment for statistical computing*. R Foundation for Statistical Computing.
- Schneider, O. D., LeChevallier, M. N., Reed, H. F., & Corson, M. J. (2007). A comparison of zinc and nonzinc orthophosphate-based corrosion control. *Journal American Water Works Association*, 99(11), 103.
- Schock, M. R. (1980). Response of Lead solubility to dissolved carbonate in drinking water. *Journal American Water Works Association*, 72(12), 695.
- Schock, M. R. (1981). Erratum: Response of Lead solubility to dissolved carbonate in drinking water. *Journal of the American Water Works Association*, 73(3), 36.
- Schock, M. R. (1989). Understanding corrosion control strategies for lead. *Journal American Water Works Association*, 81(7), 88.
- Schock, M. R., & Clement, J. A. (1998). Control of lead and copper with non-zinc orthophosphate. *New England Water Works Association*, 112(1), 20.
- Schock, M. R., & Gardels, M. C. (1983). Plumbosolvency reduction by high pH and low carbonate—Solubility relationships. *Journal American Water Works Association*, 75(2), 87.
- Schock, M. R., & Lytle, D. A. (2011). Internal corrosion and deposition control. In J. K. Edzwald (Ed.), *Water quality and treatment: A handbook of community water supplies*. McGraw-Hill.
- Schock, M. R. & Sandvig, A. M. (2004). Solubility models and their limitations. *2004 American Water Works Association annual conference*.
- Schock, M. R., & Wagner, I. (1985). The corrosion and solubility of lead in drinking water. In *Internal corrosion of water distribution systems*. American Water Works Association Research Foundation.
- Schock, M. R., Wagner, I., & Oliphant, R. J. (1996). Corrosion and solubility of lead in drinking water. In *Internal corrosion of water distribution systems* (2nd ed.). American Water Works Association Research Foundation.
- Schott, G. J. (1998). WATERPRO corrosion control and treatment process evaluation program. *Proceedings of the water quality technology conference*, San Diego, CA: American Water Works Association.
- Sheiham, I., & Jackson, P. J. (1981). The scientific basis for control of Lead in drinking water by water treatment. *Journal of the Institution of Water Engineers and Scientists*, 35, 491.
- Topolska, J., Manecki, M., Bajda, T., Borkiewicz, O., & Budzewski, P. (2016). Solubility of Pyromorphite  $Pb_5(PO_4)_3Cl$  at 5–65°C and its experimentally determined thermodynamic parameters. *The Journal of Chemical Thermodynamics*, 98, 282–287.
- Triantafyllidou, S., Burkhardt, J., Tully, J., Cahalan, K., DeSantis, M., Lytle, D., & Schock, M. (2021). Variability and sampling of Lead (Pb) in drinking water: Assessing potential human exposure depends on the sampling protocol. *Environment International*, 146, 106259.
- Tully, J., DeSantis, M. K., & Schock, M. R. (2019). Water quality–pipe deposit relationships in midwestern lead pipes. *AWWA Water Science*, 1(2), e1127.
- United States Environmental Protection Agency. (2019). *Optimal corrosion control treatment evaluation technical recommendations for primacy agencies and public water systems (EPA 816-B-16-003, dated march 2016, updated 2019)*. United States Environmental Protection Agency.

- Williams, D. J., Parrett, C. J., Schock, M. R., Muhlen, C., Donnelly, P., & Lytle, D. A. (2018). Design and testing of USEPA's Flint pipe rig for corrosion control evaluation. *Journal American Water Works Association*, 110(10), E16.
- Xie, L., & Giammar, D. E. (2007). Equilibrium solubility and dissolution rate of the lead phosphate chloropyromorphite. *Environmental Science & Technology*, 41(23), 8050.
- Zhang, Y., Griffin, A., Rahman, M., Camper, A., Baribeau, H., & Edwards, M. (2009). Lead contamination of potable water due to nitrification. *Environmental Science & Technology*, 43(6), 1890.
- Zhu, Y. N., Zhu, Z. Q., Zhao, X., Liang, Y. P., & Huang, Y. H. (2015). Characterization, dissolution, and solubility of Lead Hydroxypyromorphite  $[\text{Pb}_5(\text{PO}_4)_3\text{OH}]$  at 25–45°C. *Journal of Chemistry*, 1, 269387.

## SUPPORTING INFORMATION

Additional supporting information may be found in the online version of the article at the publisher's website.

**How to cite this article:** Wahman, D. G., Pinelli, M. D., Schock, M. R., & Lytle, D. A. (2021). Theoretical equilibrium lead(II) solubility revisited: Open source code and practical relationships. *AWWA Water Science*, e1250. <https://doi.org/10.1002/aws2.1250>